D0 Note 5651-CONF

Measurement of $Br(B_s^0 \to D_s^{(*)} D_s^{(*)})$ and the Lifetime Difference in the B_s^0 System

The D0 Collaboration
URL: http://www-d0.fnal.gov

(Dated: May 2, 2008)

We present a measurement of $Br(B_s^0 \to D_s^{(*)} D_s^{(*)})$ and derive the width difference between mass eigenstates in the B_s^0 system, $\Delta\Gamma_s = \Gamma_L - \Gamma_H$. Under certain assumptions, the final state of $B_s^0 \to D_s^{(*)} D_s^{(*)}$ is predominantly CP-even and the branching fraction measurement can be related directly to $\Delta\Gamma_s^{CP}$. The branching fraction is measured to be $Br(B_s^0 \to D_s^{(*)} D_s^{(*)}) = 0.042 \pm 0.015(\text{stat}) \pm 0.017(\text{syst})$ and the width difference is found to be $\Delta\Gamma_s/\Gamma_s = 0.088 \pm 0.030(\text{stat}) \pm 0.036(\text{syst})$ in the standard model. The result is based on a 2.8 fb^{-1} data set recorded by the D0 detector at the Fermilab Tevatron Collider.

Preliminary Results for FPCP 2008

I. INTRODUCTION

In the standard model (SM), the $B_s^0 - \bar{B}_s^0$ mixing phase $\phi_s^M \{= \arg(M_{12})\}$ can be safely neglected for a discussion of $\Delta\Gamma_s$. In this case, the mass eigenstates coincide with the CP eigenstates with $|B_L\rangle = |B_s^{even}\rangle$ and $|B_H\rangle = |B_s^{odd}\rangle$, and any $b \to c\bar{c}s$ decay into a CP-even ground state like $D_s^+ D_s^-$ arises solely from the $|B_L\rangle$ component in the untagged sample. A lifetime fit to this decay therefore determines Γ_L. However, in the presence of new physics, the CP-violating phase ϕ_s can be large and $\Delta\Gamma_s$ is diminished by a factor of $\cos\phi_s$; $\Delta\Gamma_s = \Delta\Gamma_s^{CP}\cos\phi_s$, where $\Delta\Gamma_s^{CP}\{= \Gamma_s^{even} - \Gamma_s^{odd}\}$ is insensitive to the new physics. Under various theoretical assumptions [1], the final state in $B_s^0 \to D_s^{(*)} D_s^{(*)}$ also becomes CP-even to within 5%. In this limit, the branching ratio to this final state is related to the fractional width difference by [2, 3]

$$2Br(B_s \to D_s^{(*)} D_s^{(*)}) \simeq \Delta\Gamma_s^{CP} \left[\frac{1+\cos\phi_s}{2\Gamma_L} + \frac{1-\cos\phi_s}{2\Gamma_H} \right]. \quad (1)$$

This method for measuring $\Delta\Gamma_s^{CP}/\Gamma_s$ has been exploited by ALEPH [5] using $\phi\phi$ correlations, and D0 [6] using $D_s D_s$ correlations assuming no new physics, for which $\phi_s = 0$ and $\Delta\Gamma_s^{CP}$ is equivalent to $\Delta\Gamma_s$. From these experiments the world average is $\Delta\Gamma_s/\Gamma_s = 0.096 \pm 0.048$ [4]. Within the SM framework, on the other hand, this ratio is predicted by theory [7] to be $\Delta\Gamma_s/\Gamma_s = 0.127 \pm 0.024$.

This analysis is based on a data sample corresponding to an integrated luminosity of 2.8 fb^{-1} of $p\bar{p}$ collisions collected by the D0 detector at the Fermilab Tevatron Collider between 2002 and 2007. Due to the installation of an additional layer of silicon tracker in 2006, separate measurements are performed for Run IIa (1.3 fb^{-1}) and Run IIb (1.5 fb^{-1}) and later combined. This analysis considers B_s^0 decays into two $D_s^{(*)}$ mesons and the correlation between these final state particles is examined. Here, $D_s^{(*)}$ denotes either D_s or D_s^*, since it is not possible to distinguish between them due to undetected particles in the $D_s^* \to D_s\gamma/\pi^0$ decay. We search for one $D_s^{(*)}$ decaying to $\phi\pi$ and the other decaying to $\phi\mu\nu$, where both ϕ's decay to K^+K^-. We designate the first ϕ as ϕ_1 and the second as ϕ_2. The branching ratio measurement is performed by normalizing the $B_s^0 \to D_s^{(*)} D_s^{(*)}$ sample to the $B_s^0 \to D_s^{(*)}\mu\nu$ sample:

$$\frac{N(B_s^0 \to D_s^{(*)} D_s^{(*)})}{N(D_s\mu) f(B_s^0 \to D_s^{(*)}\mu\nu)} = \frac{2 \cdot Br(B_s^0 \to D_s^{(*)} D_s^{(*)}) Br(D_s \to \phi\mu\nu) Br(\phi \to KK)}{Br(B_s^0 \to D_s^{(*)}\mu\nu)} \cdot \frac{\epsilon(B_s^0 \to D_s^{(*)} D_s^{(*)})}{\epsilon(B_s^0 \to D_s^{(*)}\mu\nu)}, \quad (2)$$

where N is the number of events in each sample, f is the fraction of events in the $D_s\mu$ sample originating from the $B_s^0 \to D_s^{(*)}\mu\nu$ decay, and ϵ is the reconstruction efficiency.

The D0 detector was designed as a general purpose detector [8] and comprises a central tracking system, a LAr-U calorimeter, and an iron toroid muon spectrometer. Charged particles are reconstructed by the tracking system consisting of a silicon microstrip tracker (SMT) and a central fiber tracker (CFT) located inside a superconducting solenoidal coil that provides a magnetic field of 2 T. Muons are reconstructed using a spectrometer located outside the calorimeter. It consists of magnetized iron toroids and three superlayers of proportional drift tubes along with scintillation trigger counters.

II. SAMPLE SELECTION

A. Common Sample

Most of the events were collected using single-muon triggers, although no explicit trigger requirement was made. Categorizing events into samples is the first stage of the analysis. We select a common sample containing muon tracks and $D_s \to \phi_1\pi$ candidates, $D_s(\phi_1\pi)$. Muons are selected with momentum requirements, $p_T > 2.0$ GeV/c and total momentum $p_{tot} > 3.0$ GeV/c. Two oppositely charged particles with $p_T > 0.7$ GeV/c are assigned the kaon mass to form a ϕ_1 meson. For each track, the transverse, ϵ_T, and longitudinal, ϵ_L, projections of the track impact parameter with respect to the primary vertex, along with the corresponding uncertainties $\sigma(\epsilon_T)$ and $\sigma(\epsilon_L)$, are computed. The significance $(\epsilon_T/\sigma(\epsilon_T))^2 + (\epsilon_L/\sigma(\epsilon_L))^2$ is required to be greater than 4 for at least one of kaons. To select signal events, the two-kaon system is required to have $p_T > 2.0$ GeV/c and $1.010 < m(KK) < 1.030$ GeV/c^2. A third particle with an opposite charge to the muon is assigned the pion mass and combined with the pair of kaons to reconstruct the $D_s(\phi_1\pi)$ system. To be accepted, the χ^2_{vtx} of the three-track vertex fit is required to be less than 16. For good $D_s(\phi_1\pi)$ candidates, the significance of the distance between the primary vertex and the D_s vertex in the transverse plane, d_T^D, is also required to be greater than 4 standard deviation, i.e. $d_T^D/\sigma(d_T^D) > 4$. The angle α_T^D between the D_s momentum and the displacement from the primary vertex to the D_s vertex in the transverse plane must satisfy

$\cos(\alpha_T^D) > 0.90$. Furthermore, the helicity angle, θ_{hel}, is defined as the angle between the D_s and one of the kaons in the KK center of mass frame, and the condition $|\cos(\theta_{hel})| > 0.30$ is imposed.

B. $D_s\mu$ Sample

A $D_s\mu$ sample is constructed by requiring the trajectory of the muon and the $D_s(\phi_1\pi)$ to originate from a common vertex. These tracks are required to have a well-reconstructed vertex by demanding $\chi^2_{vtx} < 9$ for the vertex fit. If the distance d_T^B exceeds $4 \cdot \sigma(d_T^B)$, the angle α_T^B is required to satisfy $\cos(\alpha_T^B) > 0.95$. The distance d_T^B is allowed to be greater than d_T^D, provided the distance, d_T^{BD}, between B_s^0 and D_s vertices is less than $2 \cdot \sigma(d_T^{BD})$. Isolation is defined as the momentum fraction of signal-associated tracks with respect to all tracks in a cone $\Delta R = \sqrt{(\Delta\eta)^2 + (\Delta\phi)^2} < 0.5$ around the direction of the $D_s\mu$ system. We require the isolation to be greater than 0.50. The visible proper decay length, *VPDL*, $M(B_s^0) \cdot (\vec{L}_T \cdot \vec{p}_T)/p_T^2$, is introduced to reject non-b background processes. Here $M(B_s^0)$ is the mass of the B_s^0 meson, $\vec{L}_T$ is the displacement from the primary vertex to the B_s^0 decay vertex in the transverse plane, and $\vec{p}_T$) is the total transverse momemtum vector. We require *VPDL* to exceed 150 μm. All events satisfying $p_T(D_s\mu) > 10$ GeV/c and $2.30 < m(D_s\mu) < 5.20$ GeV/c^2 are selected as the $D_s\mu$ sample.

C. $D_s\phi_2\mu$ Sample

To construct a $D_s\phi_2\mu$ sample, we search for another pair of oppositely charged particles from the common sample to form the second $\phi_2(KK)$ system. The same selection criteria as in the common sample are imposed on the kaons, except the transverse momentum $p_T(KK) > 3.0$ GeV/c is introduced to suppress fake tracks. This $\phi_2(KK)$ system is combined with the muon to produce a common vertex for the secondary D_s candidate. The χ^2_{vtx} of the three-track vertex fit is required to be less than 25. If the distance d_T^D exceeds $4 \cdot \sigma(d_T^D)$, the angle α_T^D is required to satisfy $\cos(\alpha_T^D) > 0.90$. We enhance the signal by imposing constraints of $p_T > 6.0$ GeV/c and $1.30 < m < 1.85$ GeV/c^2 on the $D_s \to \phi_2\mu$ system, $D_s(\phi_2\mu)$. The $D_s(\phi_1\pi)$ and $D_s(\phi_2\mu)$ are required to originate from a common vertex to reconstruct B mesons. To reduce many systematic uncertainties, we apply the same selection criteria to these B_s candidates as in the $D_s\mu$ sample except the mass constraint. All events whose total invariant mass lies between 4.30 and 5.20 GeV/c^2 are categorized as the $D_s\phi_2\mu$ sample.

D. Combined Tagging Variable

The final sample selection is performed by utilizing a likelihood ratio method [9]. For a set of discriminating variables, the probability density functions (PDFs) are built from the signal region and from background sidebands. The sidebands are background regions adjacent to the signal and of a half mass width of the signal. The ratio of these PDFs is calculated for each variable and then combined to produce the combined tagging variable. The requirement on this variable is determined by demanding the maximal value of $S/\sqrt{S+B}$, where S and B are the number of signal and background events.

III. FITTING PROCEDURE

A binned likelihood fit is chosen for the $D_s\mu$ sample and all events with $1.70 < m(D_s(\phi_1\pi)) < 2.30$ GeV/c^2 are used in the fit. The resulting $D_s(\phi_1\pi)$ and $\phi_1(KK)$ invariant mass distributions are shown in Fig. 1. The number of $D_s\mu$ events is extracted assuming possible contributions from $D^{\pm}$ and D_s as signal and from combinatorial backgrounds. The fit gives $N(D_s\mu) = 28,680 \pm 288$.

The correlation between $D_s(\phi_1\pi)$ candidates and $\phi_2(KK)$ candidates can be exploited in a two-dimensional unbinned likelihood fit. All events with $1.70 < m(\phi_1\pi) < 2.30$ GeV/c^2 and $0.980 < m(KK) < 1.070$ GeV/c^2 are included in the fit. In this procedure, all mean mass and width parameters of the PDFs for both $D_s(\phi_1\pi)$ and $\phi_2(KK)$ are fixed to the values obtained from the $D_s\mu$ sample, while all parameters of the background functions are left unconstrained. Fig. 2 shows the result of the fit for the signal and background, where the fit yields $N(D_s\phi_2\mu) = 31.0 \pm 9.4$. The statistical significance is calculated to be 3.7 σ based on the change in the likelihood when we fit the entire data set with and without a signal. For a consistency check, a binned likelihood fit is also implemented on the same sample by looking at one system at a time. $N(D_s\phi_2\mu) = 31.2 \pm 10.7$ is obtained from the $\phi_1\pi$ mass fit, while

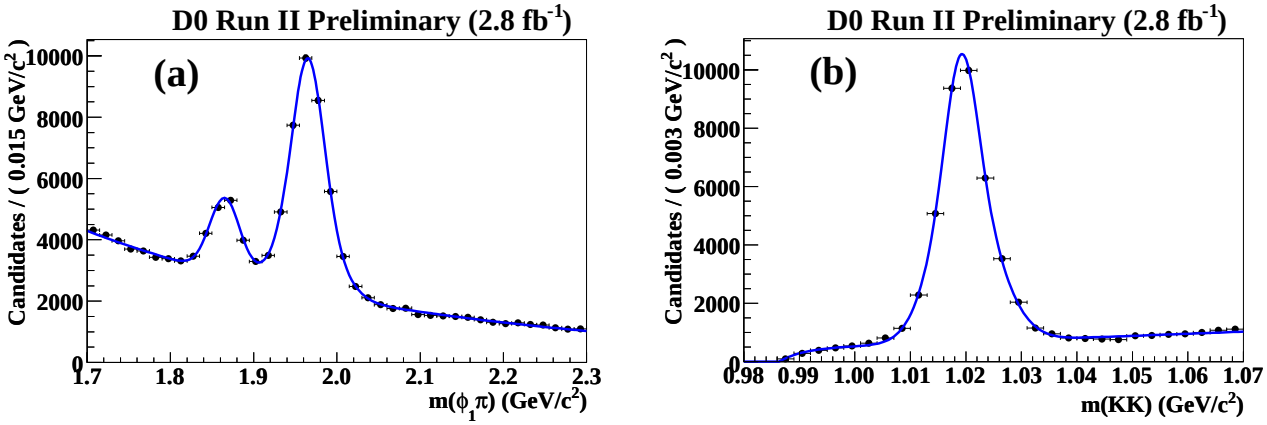

FIG. 1: Invariant mass distributions for the $D_s\mu$ sample. (a) $m(\phi_1\pi)$ spectrum from the KK signal region, $1.01 < m(KK) < 1.03$ GeV/c^2. The two peaks represent the $D^{\pm} \to \phi\pi$ (left) and the $D_s \to \phi\pi$ (right). (b) $m(KK)$ spectrum from the $m(\phi_1\pi)$ signal region, $1.92 < m(\phi_1\pi) < 2.00$ GeV/c^2.

$N(D_s\phi_2\mu) = 31.7 \pm 11.3$ are observed from the KK mass fit. These numbers are consistent with the results from the unbinned likelihood fit.

IV. SAMPLE COMPOSITION

A. $D_s\mu$ Sample

The fraction $f(B_s^0 \to D_s^{(*)}\mu\nu X)$ is extracted by analyzing the $D_s\mu$ sample. Treating $B_s^0 \to D_s^{(*)}\mu\nu X$ decay as signal, the following decay processes are considered as background: $B^0 \to D_s^{(*)}D^{(*)}X$, $B^{\pm} \to D_s^{(*)}D^{(*)}X$, $B_s^0 \to D_s^{(*)}D^{(*)}X$, $B_s^0 \to D_s^{(*)}D_s^{(*)}$, with $D^{(*)} \to \mu\nu X$, and $B_s^0 \to D_s^{(*)}\tau\nu X(\tau \to \mu\nu\nu)$. These channels are simulated using the D0 standard Monte Carlo (MC) tools and reconstructed using the same algorithms as for data. In addition to these processes, the peaking background, which consists of events originating from non-B mesons and is dominated by $c\bar{c}$ production, is also taken into account. The $c\bar{c}$ contribution to the $B_s^0 \to D_s^{(*)}\mu\nu X$ sample, $f_{c\bar{c}}(c\bar{c} \to D_s^{(*)}\mu\nu)$, is estimated to be (10.3 ± 2.5) % and the *VPDL* distribution is a Gaussian centered at zero [11]. Based on these two results, the $c\bar{c}$ contribution with the requirement of $VPDL > 150$ μm is estimated to be (1.9 ± 0.5) %. After all cuts, the signal fraction in the $D_s\mu$ sample is estimated by

$$f(B_s \to D_s^{(*)}\mu\nu) - f_{c\bar{c}}(c\bar{c} \to D_s^{(*)}\mu\nu) = \frac{1}{1 + \sum_i r_i},$$

where r_i is the ratio of the efficiency for the individual background processes to the efficiency for the total signal processes $B_s \to D_s\mu\nu X$.

B. $D_s\phi_2\mu$ Sample

The number of candidates, $N(D_s^{(*)}D_s^{(*)})$ and $N_{c\bar{c}}(D_s^{(*)}D_s^{(*)})$, are determined from the $D_s\phi_2\mu$ sample decomposition. Considering $B_s^0 \to D_s^{(*)}D_s^{(*)}$ as the signal process, the following are background processes: 1) $B_s^0 \to D_s^{(*)}D_s^{(*)}X$, 2) $B^{\pm,0} \to D_s^{(*)}D_s^{(*)}X$, 3) $B_s^0 \to D_s^{(*)}\mu\nu\phi$, 4) $B_s^0 \to D_s^{(*)}\mu\nu$ + uncorrelated ϕ from fragmentation, and 5) peaking background. The first background component consists of the B_s^0 multi-body double charm decays that are not CP eigenstates and have not been explicitly observed experimentally. Two possible final states are $D_s^{(*)}D_s^{(*)}(n)\pi$ and $D_s^{(*)}D_s^{(*)}\phi$. Under isospin conservation, the first decay requires at least two pions in the final state, which requires two gluons, as in $\psi' \to J/\psi\pi\pi$. Therefore these decays are strongly suppressed. The second background from B decays producing an $s\bar{s}$ meson in the final state are also negligible with the requirement of $m(D_s\phi_2\mu) > 4.30$ GeV/c^2. In addition, B multi-body decays can affect the sample composition. Since the $D \to \phi X$ decays are Cabbibo- and color-suppressed in contrast to $D_s \to \phi X$, the possible decay contains a kaon in the final state. A large portion of

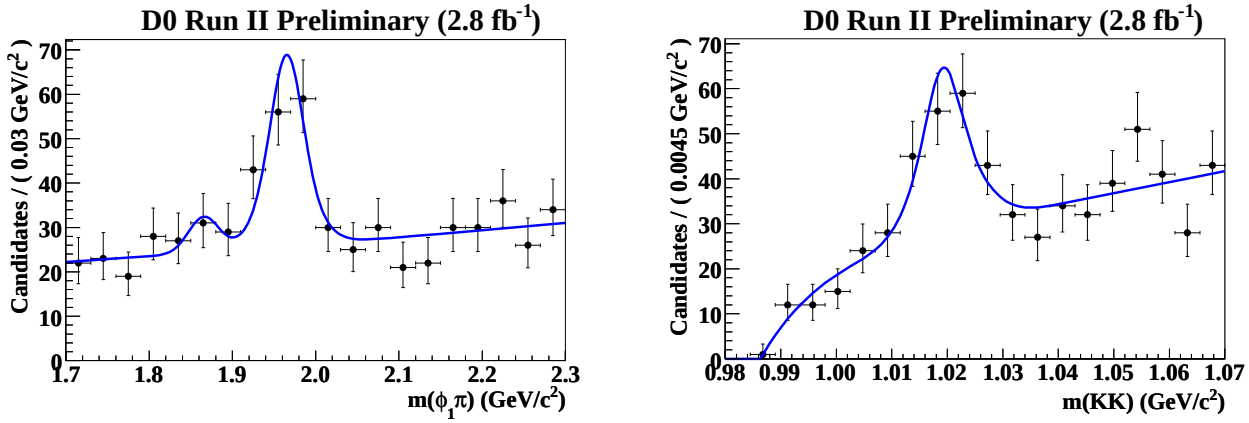

FIG. 2: Invariant mass distributions for the $D_s\phi_2\mu$ sample - (a) $m(\phi_1\pi)$ spectrum and (b) $m(KK)$ spectrum. The correlation between $D_s(\phi_1\pi)$ and $\phi(KK)$ is exploited by the two-dimensional unbinned likelihood fit.

these decays, however, can be removed by the mass cut on the $D_s\phi_2\mu$ system. The third background component yields a high mass distribution in the $D_s(\phi_2\mu)$ system. Therefore a mass cut of $m(\phi_2\mu) < 1.85$ GeV/c^2 reduces its contamination. In the fourth background the production of a ϕ meson from fragmentation accompanied by a $B_s^0 \to D_s^{(*)}\mu\nu$ decay could also fake the signal events. Such events are entirely rejected by requiring $VPDL > 150\ \mu m$. The fifth background from the $c\bar{c} \to D_s^{(*)}D_s^{(*)}X$ contribution can be calculated from the $c\bar{c}$ contribution in the $D_s\mu$ sample, $f_{c\bar{c}}$, by the relation

$$\frac{N_{c\bar{c}}(D_s\phi_2\mu)}{N(D_s\mu)f_{c\bar{c}}(D_s\mu)} = \frac{Br(c\bar{c} \to D_s\phi_2\mu)}{Br(c\bar{c} \to D_s\mu)} \cdot \frac{\epsilon(c\bar{c} \to D_s\phi_2\mu)}{\epsilon(c\bar{c} \to D_s\mu)},$$

where $N_{c\bar{c}}$ is the number of $c\bar{c}$ events and ϵ is the reconstruction efficiency. An estimate of 0.51 ± 0.54 events and 0.39 ± 0.41 events is obtained for the $c\bar{c}$ contribution in the $D_s\phi_2\mu$ sample for Run IIa and Run IIb.

The signal fraction of $B_s^0 \to D_s^{(*)}D_s^{(*)}$ in the $D_s\phi_2\mu$ sample is estimated by assuming the background is dominated by the two processes: $B^{\pm,0} \to D_s^{(*)}D_s^{(*)}KX$ and $B_s^0 \to D_s^{(*)}\mu\nu\phi$. Fig. 3 shows a two-dimensional mass distribution of the two systems, $m(\phi_2\mu)$ and $m(D_s\phi_2\mu)$, for each decay process. We divide the plot into nine different regions according to selection cuts made to the $D_s\phi_2\mu$ sample and take into account three regions labeled 1, 2, and 3. We define M_i as the total number of events in the sample for channel i and n_j as the number of events in region j, which can be obtained from the fitting procedure. Defining $f_{i,j}$ as the fraction of events in the j region being occupied by the channel i, which can be estimated from the MC sample, the following equation is applicable in region i:

$$n_j = f_{a,j} \cdot M_a + f_{b,j} \cdot M_b + f_{c,j} \cdot M_c,$$

where the channel a corresponds to the $B_s^0 \to D_s^{(*)}D_s^{(*)}$ decay, b to the $B^{\pm,0} \to D_s^{(*)}D_s^{(*)}KX$ decay, and c to the $B_s^0 \to D_s^{(*)}\mu\nu\phi$ decay. Finally, a 3×3 matrix equation can be constructed as

$$\begin{pmatrix} n_1 \\ n_2 \\ n_3 \end{pmatrix} = \begin{pmatrix} f_{a,1} & f_{b,1} & f_{c,1} \\ f_{a,2} & f_{b,2} & f_{c,2} \\ f_{a,3} & f_{b,3} & f_{c,3} \end{pmatrix} \begin{pmatrix} M_a \\ M_b \\ M_c \end{pmatrix}.$$

By solving this matrix equation, the number of $D_s^{(*)}D_s^{(*)}$ events can be expressed as $N(D_s^{(*)}D_s^{(*)}) = f_{a,1} \cdot M_a$ and the number of $c\bar{c}$ events as $N_{c\bar{c}}(D_s^{(*)}D_s^{(*)}) = N_{c\bar{c}}(D_s\phi_2\mu) \cdot (f_{a,1} \cdot M_a)/\sum_i (f_{i,1} \cdot M_i)$, where $i = a,\ b,\ c$. Then the number of pure signal events is given by $N(B_s^0 \to D_s^{(*)}D_s^{(*)}) = N(D_s^{(*)}D_s^{(*)}) - N_{c\bar{c}}(D_s^{(*)}D_s^{(*)})$. The statistical errors in n_2, n_3, and $N_{c\bar{c}}(D_s^{(*)}D_s^{(*)})$ are taken into account as systematic uncertainties.

V. OTHER COMPONENTS

The reconstruction efficiency is estimated through a MC study. We generate exclusive samples for $B_s^0 \to D_s^{(*)}\mu\nu$ and $B_s^0 \to D_s^{(*)}D_s^{(*)}$ and apply the same fitting procedure as for the data sample, except removing the $D^{\pm} \to \phi\pi$. The

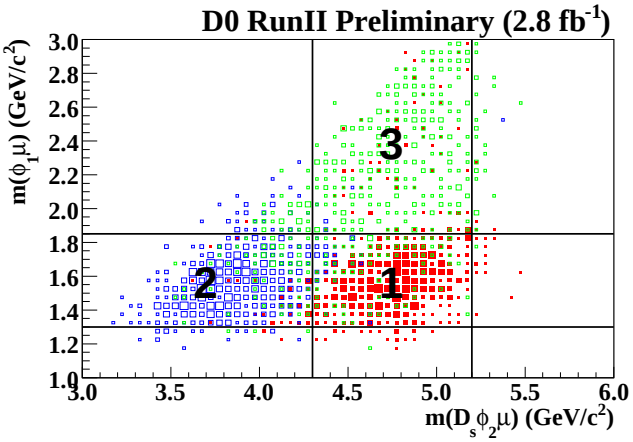

FIG. 3: Two dimensional plot of $m(\phi_2\mu)$ vs. $m(D_s\phi_2\mu)$. The signal channel $B_s^0 \to D_s^{(*)}D_s^{(*)}$ is represented by red (dark) dots while two background channels, $B^{\pm,0} \to D_s^{(*)}D_s^{(*)}KX$ and $B_s^0 \to D_s^{(*)}\mu\nu\phi$, are represented by blue (dark) and green (bright) boxes respectively. The regions labeled 1, 2, and 3 as in (b) are dominated by a particular decay channel.

resulting estimate of the ratio of reconstruction efficiencies, $\epsilon(B_s^0 \to D_s^{(*)}D_s^{(*)})/\epsilon(B_s^0 \to D_s^{(*)}\mu\nu)$, is (8.7 ± 1.5) % for Run IIa and (8.0 ± 1.5) % for Run IIb. This measurement also requires branching ratios which we take from the current PDG [10]: $Br(B_s^0 \to D_s^{(*)}\mu\nu) = 0.079 \pm 0.024$, $Br(D_s \to \phi\mu\nu) = 0.0249 \pm 0.0028$, and $Br(\phi \to K^+K^-) = 0.493 \pm 0.006$.

VI. SYSTEMATIC UNCERTAINTIES

The main systematic uncertainty arises from the precision in the branching ratio measurements from the PDG [10]. They are allowed to vary within one standard deviation to obtain the systematic uncertainty. $Br(B_s^0 \to D_s^{(*)}\mu\nu) = 0.079 \pm 0.024$ is the dominant source which gives a > 50 % contribution to the total systematic uncertainty. The $Br(D_s \to \phi\mu\nu) = 0.0249 \pm 0.0028$ also contributes to the uncertainty. The uncertainty of the reconstruction efficiency ratio comes from the weighting process to the MC samples to account for the trigger effect. We calculate its error from the difference in measurements between with and without the trigger efficiency curve applied to the samples. The fitting procedure in the $D_s\phi_2\mu$ sample is responsible for a systematic uncertainty by forcing all signal PDF parameters to be fixed. We free all parameters in the $D_s(\phi_1\pi)$ system and follow the same procedure, then we estimate its contribution as difference between two approaches. The matrix method used in the $D_s\phi_2\mu$ sample decomposition gives rise to another uncertainty. The error in this calculation results from the lack of statistics due to the small sample size. Contributions to the systematic uncertainty from the estimation of the fraction, f, and the peaking background are negligible.

TABLE I: Summary of systematic uncertainties.

Source	Uncertainty
$Br(B_s \to D_s^{(*)}\mu\nu)$	0.0127
$Br(D_s \to \phi\mu\nu)$	0.0047
$Br(\phi \to KK)$	0.0006
$\epsilon(D_s^{(*)}D_s^{(*)})/\epsilon(D_s^{(*)}\mu\nu)$	0.0072
fitting procedure	0.0071
$N(D_s^{(*)}D_s^{(*)})$ (Matrix)	0.0041
$N(D_s\mu)$	0.0005
$f(B_s \to D_s^{(*)}\mu\nu)$	0.0006
$c\bar{c}$ background	0.0011
Total	0.0174

VII. RESULT AND CONCLUSION

Using all these inputs, we obtain the branching ratio from Eq. (2):

$$Br(B_s^0 \to D_s^{(*)} D_s^{(*)}) = 0.042 \pm 0.015(\text{stat}) \pm 0.017(\text{syst}).$$

The systematic uncertainty could be significantly improved by a more precise measurement of the branching ratio $Br(B_s^0 \to D_s^{(*)} \mu\nu)$. Assuming Eq. (1) is applicable under certain theoretical assumptions and allowing for no new physics, we obtain

$$\frac{\Delta\Gamma_s}{\Gamma_s} = 0.088 \pm 0.030(\text{stat}) \pm 0.036(\text{syst}).$$

This result is consistent with the SM prediction [7] where CP violation in B_s^0 mixing is assumed to be small.

Acknowledgments

We thank the staffs at Fermilab and collaborating institutions, and acknowledge support from the DOE and NSF (USA); CEA and CNRS/IN2P3 (France); FASI, Rosatom and RFBR (Russia); CNPq, FAPERJ, FAPESP and FUNDUNESP (Brazil); DAE and DST (India); Colciencias (Colombia); CONACyT (Mexico); KRF and KOSEF (Korea); CONICET and UBACyT (Argentina); FOM (The Netherlands); STFC (United Kingdom); MSMT and GACR (Czech Republic); CRC Program, CFI, NSERC and WestGrid Project (Canada); BMBF and DFG (Germany); SFI (Ireland); The Swedish Research Council (Sweden); CAS and CNSF (China); and the Alexander von Humboldt Foundation.

[1] R. Aleksan *et al.*, Phys. Lett. B **316**, 567 (1993).
[2] K. Anikeev *et al.*, arXiv:hep-ph/0201071 (2002).
[3] I. Dunietz, R. Fleischer, and U. Nierste, Phys. Rev. D **63**, 114015 (2001).
[4] E. Barberio *et al.* (Heavy Flavor Averaging Group), arXiv:0704.3575 [hep-ex] (2007).
[5] R. Barate *et al.* (ALEPH Collaboration), Phys. Lett. B **486**, 286 (2000).
[6] V.M. Abazov *et al.* (D0 Collaboration), Phys. Rev. Lett. **99**, 241801 (2007).
[7] A. Lenz and U. Nierste, J. High Energy Phys. **0706**, 072 (2007).
[8] V.M. Abazov *et al.* (D0 Collaboration), Nucl. Instrum. Methods A **565**, 463 (2006).
[9] G. Borissov, Nucl. Instrum. Methods Phys. Res. A **417**, 384 (1998).
[10] W.-M. Yao *et al.*, Journal of Physics, G **33**, 1 (2006) and 2007 partial update for 2008.
[11] V.M. Abazov *et al.* (D0 Collaboration), Phys. Rev. Lett. **94**, 182001 (2005).